

A simple numerical method for the earthquake response analysis of surface ground

Jingzhe Zheng

Kajima Technical Research Institute, Kajima Corporation, Japan

Choshiro Tamura

The University of Tokyo, Japan

ABSTRACT: This paper presents a numerical method for the earthquake response analysis of surface ground. The proposed method proceeds by directly tracing wave front propagation in time domain, having very simple algorithm with short calculation time and small memory storage. By using the proposed method, the responses of soft deposit with irregular shape of basement are studied, and compared with the response of a deposit with a horizontal basement. The nonlinear behavior of a deposit with a thin soft layer located inside is also analyzed.

1 INTRODUCTION

Investigations of the earthquake damage (e.g., JSCE, 1986) have revealed that local ground structures largely affect the earthquake response characteristics at the surface. During these years, in order to apprehend the effects of local site conditions on the seismic motion at the surface, a number of experimental studies (e.g., Tamura and Suzuki, 1988), theoretical investigations (e.g., Aki and Larnier, 1970; Bard and Bouchon, 1985; Trifunac, 1990) and observed earthquake response analysis (e.g., Okamoto, 1973) have been carried out. These previous studies have shown the importance of geological irregularities and local soil conditions. However, there are still many unsolved problems because of the lack of observed data and the complexity of numerical analysis. This paper attempts to present a simple numerical analysis method, and investigate the effects of local conditions on the earthquake response of soft deposit. Main attention is paid to the comparison between the responses of soft surface deposits with and without geological irregularity. The example of nonlinear analysis is also shown. SH wave incidence case is treated.

2 DESCRIPTION OF THE WAVE FRONT TRACING METHOD

Our method (Zheng et al., 1989) proceeds in two steps. First, we input a unit impulse wave from the basement. Because of reflections and refractions at boundaries between different media, the number of im-

pulses increases, and the amplitude of impulses changes. Impulse amplitude variations are calculated by using reflective and refractive coefficients, which we can obtain from the impedance ratio and incident angle. The travel time of impulses are acquired by tracing rays. Through the above calculations, we can easily obtain impulse time series arriving at observation point (Fig. 1). Second, based on the impulse time series, we compute the response at the observation point for any kinds of input.

input: $a(t)$

$$\text{response: } \sum_{k=1}^n A_k f(t-t_k), \quad f(t-t_k) = \begin{cases} 0, & t < t_k \\ a(t-t_k), & t \geq t_k \end{cases} \quad (1)$$

And through the Fourier transform of the impulse time series, we derive the transfer function as

$$\sum_{k=1}^n A_k e^{i\omega t_k} \quad (2)$$

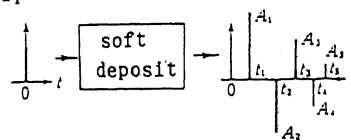


Fig.1 Calculation of impulse time series

The intrinsic attenuation is considered by using $\exp(-\alpha r)$ where $\alpha = 2h/\sqrt{(1-h^2)}L$ and r is the propagation distance, L the wavelength and h the damping ratio. When considering the damping effect, we use $A_k \exp(-\alpha r_k)$ instead of A_k in eq(1) and eq(2).

where r_k is the propagation distance of impulse. As for diffractive waves, we approximate wave amplitude by using the Fresnel integral (Zheng et al., 1989).

In the case of nonlinear analysis, we trace wave propagation time step by time step. At each time step, we compute the ground displacement and then the strain by superimposing all the waves propagating at the time. Based on the strain-stress relation, the wave velocity for the next time step can be determined. By repeating above procedure, we get the response in time domain.

The proposed method has been verified both by finite difference method (Zheng et al., 1989) and by simulating observed response of soft deposit in Tokyo bay (Zheng et al., 1992).

3 ANALYSIS OF EARTHQUAKE RESPONSE OF SOFT SURFACE GROUND

In this section, first, we will investigate the response property of soft deposit with a dipping basement and that with concave basin-shaped basement by comparing them with those of grounds overlaying a horizontal basement, and then analyze the nonlinear response of a deposit with a thin soft layer located inside.

3.1 Response of soft deposit with a dipping basement

The first model is a soft deposit with a dipping basement as shown in Fig.2. The impedance ratio between soft deposit and hard basement is 1/6, and plane SH wave is vertically incident from the basement. A is

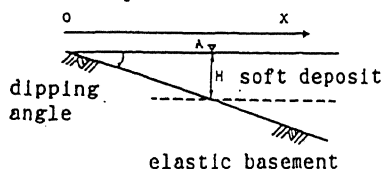


Fig.2 Analytical model of a soft deposit with a dipping base

an arbitrary observation point at the free surface with thickness of H. Now, we investigate the relationship between dipping angle and the pattern of impulse time series arriving at the A point. After a unit impulse is incident from the basement, it repeats reflection and refraction inside the soft deposit, and at last, propagate in a direction of the dip. The number of impulses arriving at the surface decreases as the dip angle of the base increases. The relationship between the number of the impulse and the dip angle can be expressed by

$$\pi/4(N-1) > \theta > \pi/4N \quad (3)$$

where θ is the dipping angle, and N the number of impulses.

The number, amplitudes and time interval of impulses vary with the dipping angle. Fig. 3 shows the impulse time series when dipping angles are 10°, 18° and 30°, respectively. The results for a horizontal base case with the surface layer thickness of H are compared by broken line in the same figure. The horizontal axis indicates the dimensionless time t/T , where T is the time interval of impulses for horizontal base case. The time durations between adjacent impulses are shorter than the case with horizontal basement, and the time durations become smaller and smaller along with time axis. These indicate that the ground with a dipping base largely amplifies the higher frequency components of input waves. We can also see that impulse time series pattern depends on the dipping angle.

T: half of the fundamental period of the case with horizontal base

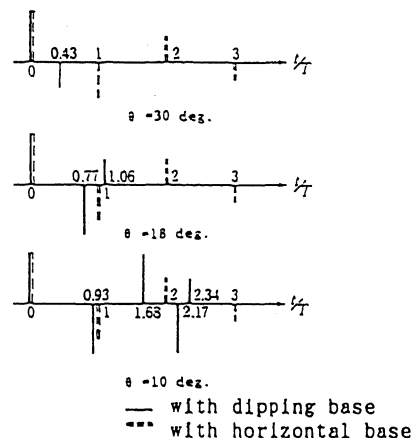


Fig.3 Comparison of impulse time series patterns

Knowing the impulse time series, we can obtain the transfer function of the surface ground and the response in time domain for arbitrary input. The transfer function for the case with the dipping angle of 30° (damping coefficient 5% & 20%) is shown in Fig.4. Horizontal axis is the dimensionless frequency $\omega x/V$, where x is the distance from the merged point and V the shear wave velocity. $\omega = 2\pi f$, where f represents wave frequency. Vertical axis indicates the amplification ratio. When damping coefficient is 5%, the amplification ratio of the case with dipping base obviously differs from that with a horizontal base. In the case that the damping ratio is 20%, however, the distinction between the two cases be-

comes much smaller. It worths noting that, if the predominant $\omega x/V$ of input wave is within the frequency range where the difference between transfer function of ground with horizontal base(1-D) and that with dipping base(2-D) is significant, 2-D and 1-D ground will behavior quite differently.

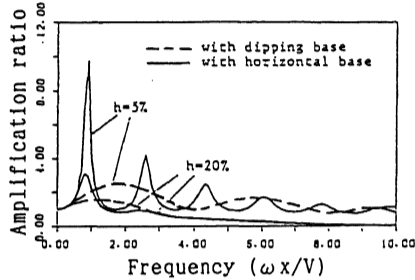


Fig.4 Comparison between the transfer function of ground with a dipping base and that with a horizontal base

3.2 Response of deposit with concave basin-shaped basement

The response properties of deposit with concave basin-shaped basement, as shown in Fig.5, will be discussed. The plane SH wave is vertically incident from the basement, and the basement is rigid. Here, main attention is given to the evaluation of the

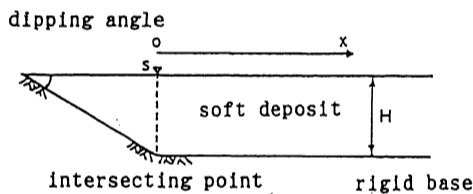


Fig.5 Analytical model of a soft deposit with a concave basin-shaped rigid base

extent of the area affected by the dipping base. To this end, we use the transfer function difference index(Zheng et al., 1990), which is defined as

$$\sum_k \text{ABS}(f_{\text{Ir}} - f_{\text{H,k}}) \Delta f / \sum_k f_{\text{H,k}} \Delta f \quad (4)$$

where f_{r} represents the transfer function of ground with irregular shape of basement, f_{H} indicates that with horizontal basement. To make the index have more practical meanings, the transfer functions used are filtered first as shown in Fig. 6, taking the velocity response spectrum for the earthquake resistance design into account. Here, we use the above index to evaluate the effects of the dipping angle on the response at the free surface.

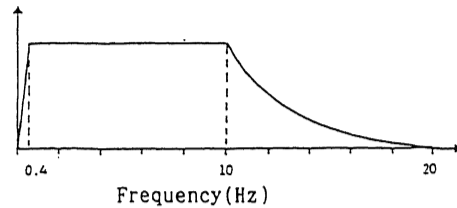


Fig.6 Pass filter used for the calculation of the transfer function difference index

We first discuss the analyzed results for the case when dipping angle is 30° and thickness is 30 m. In Fig. 7, the thick line denotes the transfer function of the point S, which is the observation station above the intersecting point of dipping basement and horizontal basement, and the thin line represents the result of horizontal basement case with surface layer thickness of H. If x (the distance from S point) increases, the transfer function of ground with concave basin-shaped basement will change. The distribution of the transfer function difference index along with the x axis is shown by solid line in Fig.8. The transfer function difference index decreases as the distance x increases. It can also be seen that transfer function index distribution is not smooth in the region where x/H is less than 1.0, which is considered as one of the characteristics of the effects resulting from the dipping base. To comprehend the effects of the dipping angle, the index distributions for the case with dipping angle of 10° (case 1) is also shown in Fig.8. The case with dipping angle of 30° is defined as case 2. From the figure, it can be seen that index value for the case 2 is larger than that of case 1 when x/H is smaller than 2.2, and the index for the two cases tend to be the same value if x/H is larger than 2.2. Similar results were obtained from the comparisons of the index distributions for other dipping angles. Thus, we can infer that the large dipping angle has large effects when x is small, and the effects of different dipping angles are similar in the region where $x/H < 2.2$.

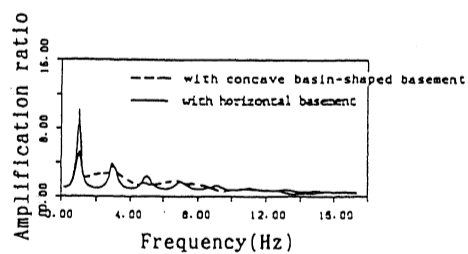


Fig.7 Comparison between transfer function of S point for ground model with concave basin-shaped base and that with a horizontal base

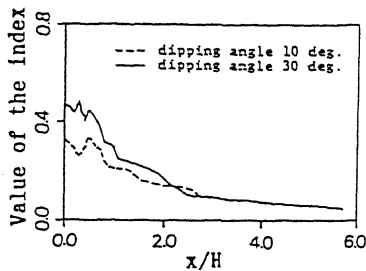


Fig.8 Distribution of the transfer function difference index along with x axis.

3.3 Example of nonlinear response analysis

The response of surface ground with a thin soft layer interspersed inside, as shown in Fig.9(a), is to be studied. In respect to the strain-stress relation of ground material, bi-linear model is adopted, and the elastic limitation strain is set as 10^{-3} . According to the results of the linear analysis, the fundamental frequency of the ground is 1.547Hz. In order to investigate the nonlinear behavior of the ground, we input Rickler Wavelet(displacement wave), with characteristic frequency of 1.547Hz, from the basement. We considered three levels of input, with maximum amplitude of 0.06cm, 0.09cm and 0.12cm, respectively. Fig.9(b) shows the maximum strain distribution of ground. The maximum strain is less than 10^{-3} in the case of level 1, and larger than 10^{-3} in the case of level 2 and level 3. As the input level increases, the strain at thin soft layer becomes larger, while the strain near the thin soft layer decreases relatively. The similar trend has been observed from other case studies.

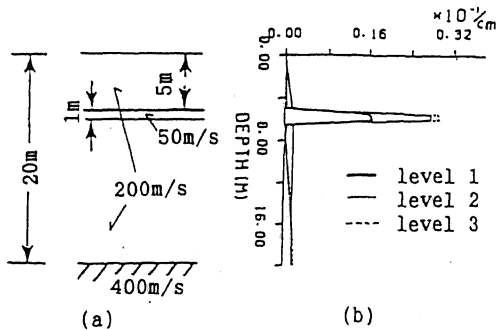


Fig.9 (a) Ground model; (b) Maximum strain distribution (divided by the amplitude of input wave)

4 CONCLUSIONS

From above analysis, the following conclusions are drawn:

- 1) Proposed method proved to be a good approach for the analysis of surface ground, which has simple algorithm with very short CPU time and memory storage.
- 2) Dipping basement largely affects the response at surface. The degree of difference between the response of ground with a dipping base and that with horizontal base depends on the dimensionless predominant frequency ($\omega x/V$) range of the input wave, damping ratio and dipping angle. If the predominant $\omega x/V$ is in the range where the difference between the transfer functions of these two grounds is large, they will perform very differently.
- 3) In case of ground with concave basin-shaped basement, the effects of dipping basement become smaller as the horizontal distance from the intersecting point of dipping base and horizontal base increases. In the area where x/H is less than 2.2, larger dipping angle is more effective. In the region $x/H > 2.2$, response does not depend on the dipping angle.

REFERENCES

- Aki, K. & K.L.Larner 1970. Surface motion of a layered medium having an irregular interface due to incident plane SH waves. *J. Geophys. Res.* 75: 933-954.
- Bard, P.Y. & M. Bouchon 1985. The two-dimensional resonance of sediment-filled valleys. *Bull. Seismol. Soc. Am.* 75: 519-541.
- JSCE 1986. Damage report of the Nihon-kai Central Part Earthquake in 1983. JSCE: Tokyo.
- Okamoto, S. 1973. Introduction to earthquake engineering. The University of Tokyo press.
- Tamura, C. & T. Suzuki 1988. Proposal of a mathematical model for earthquake response analysis of irregularly bounded surface layer. *Proc. of ninth world conference on earthquake engineering*: 665-670.
- Trifunac, M.D. 1990. How to model amplification of strong earthquake motions by local soil and geologic site conditions. *Earthq. Eng. Struc. dyn.* 19: 833-846.
- Zheng, J., C.Tamura & K.Konagai 1989. A method for earthquake response analysis of surface ground by tracing wave front. *Seisan-kenkyu*, J. IIS, the University of Tokyo 41: 922-925.
- Zheng, J., C.Tamura & K.Konagai 1990. Extent of area affected by a dipping basement. *Proc. of annual convention of JSCE*: 1128-1129.
- Zheng, J., C.Tamura & K.konagai 1992. Earthquake response analysis of ground surface by wave front tracing method. *J. Phys. Earth* 40 (in press).